

Evaluation of Naturally Fractured Reservoir Characteristics Utilizing Well Testing Analysis: A Case Study Ellenberger Oil Field

Ghassan H. Ali, Mohammed J. Zeinalabideen, Mohammed Adil Ismail, Diary N. Fattah

Department of Petroleum Engineering, University of Kirkuk, Kirkuk, Iraq

Abstract: Naturally fractured reservoirs differ significantly from conventional reservoirs due to the presence of fractures that promote fluid flow and reservoir connectivity. This study used dual-porosity and dual-permeability models to analyze well data from the Ellenberger field in Texas, USA. Dual-porosity systems simplify the complexities of fractured reservoirs with natural gaps, including fractures, and caverns, by dividing them into two basic systems - a fluid-conducting network and a storage matrix. The conductive network enhances fluid transport, while both media serve as effective fluid storage. The models developed are characterized by marked variations in their conceptual assumptions regarding the fluid flow mechanism across the matrix. The current models are based on matrix blocks of regular shapes, for instance cylinders, cubes, and spheres, and suppose that fluid exchange between the matrix and fractures arises under pseudo-steady state or unsteady conditions. In the present oil field, well tests, such as pressure buildup and drawdown, based on diffusion equations, have been performed to characterize naturally fractured reservoirs. A mathematical model was developed based on well pressure data during production, with shut-in periods analyzed to evaluate reservoir behavior accurately. The results showed that the fractures in this field classify it as Type I, where fractures play a vital role in providing porosity and permeability to the reservoir, as well as wide drainage zones per well and rapid production decline rate.

Keywords: Dual permeability; Dual porosity; Heterogeneous reservoirs; Storage capacity; Production.

1. Introduction

A naturally fractured reservoir is a type of reservoir characterized by rocks exposed to geomechanical processes that result in fractures. These fractures occur when differential forces acting on the rock exceed its elastic limits, leading to rupture. As a result of these processes, the reservoir consists of two main components: the matrix and fractures. The majority of the oil world reserves are located in naturally fractured carbonate reservoirs, which are characterized by a complex and heterogeneous porosity system. Warren and Root ^[1] presented the significance of dual porosity performance in the oil and Gas industry, developing an idealized analytical model for the flow of monophasic compressible fluids within heterogeneous reservoirs. Figure (1) shows the reservoir is represented in the model using rectangular cubes that reflect the blocks of the matrix, while the spaces between them represent the fractures. According to the model, fractures have high permeability and low storage capacity, while the matrix has high storage capacity with low permeability. The fluid flow occurs primarily through the fracture network, while the matrix supplies the stored fluids. It is also assumed that flow between the matrix and fractures occurs in a pseudo-steady state, enhancing a deeper understanding of fluid behavior within these reservoir systems.

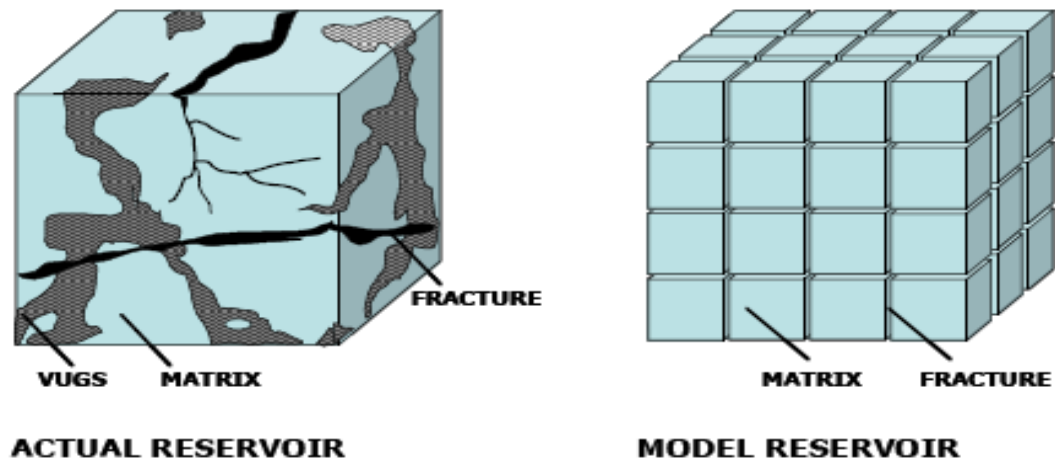


Figure 1. A Model for a Naturally Fractured Reservoir^[1]

Warren and Root [1] supposed that using the same parameters as homogeneous reservoirs, fractured reservoirs can potentially be modeled two further parameters that take into account effect of fractures. They demonstrated that the pressure transient behavior of such a reservoir exhibits a characteristic behavior, represented by the appearance of two parallel straight lines on a semi-logarithmic scale. Later, Kazemi [2] introduced a model comparable to Warren and Root [1], based on the concept of transient flow between pores within the rock matrix. Kazemi utilized numerical solutions to analyze the pressure response in a closed circular reservoir containing a central well, assuming all fractures are horizontal. An idealized representation of Kazemi's [2] model, which is based on unsteady monophasic flow in both the radial and vertical directions as shown in Figure (2). The model focuses on the movement of fluids from the matrix of rock that has high storage capacity and low permeability, to the fractures, which have low storage capacity and high permeability, creating complex hydrodynamic behavior that affects the pressure response of the system.

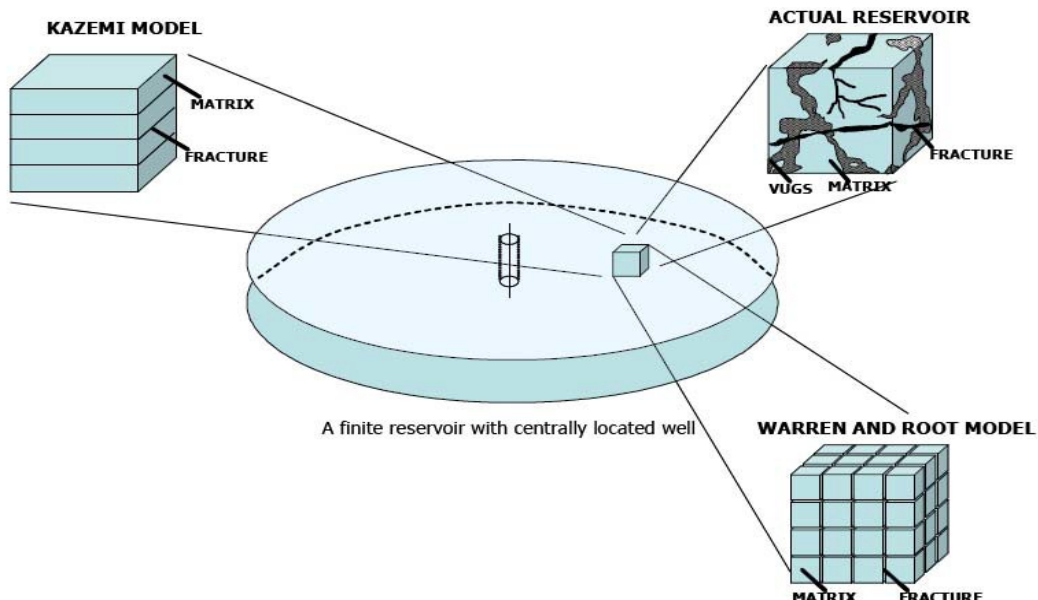


Figure 2. Naturally Fractured Reservoir^[2]

The extracted solutions resulted in three parallel straight lines on a semi-logarithmic scale. The first and third lines correspond to the behavior of Warren and Root [1]; at the same time, the resulting solutions are close to the results of Warren and Root [1], with the main difference being the phase transition between fluid flow within the fractures and the overall system flow, which is represented by the second semi-logarithmic line. Kazemi [2] confirmed the continued validity of the Warren and Root [1] model for describing unsteady flow in naturally fractured reservoirs, emphasizing that the interpore flow coefficient value depends on the mechanism of fluid migration from the rock matrix to the fractures, reflecting the complexity of hydrodynamic interactions within the reservoir. De Swaan [3] developed an analytical model for dual porosity to describe dual porosity, including the effect of transient flow within the matrix, using a different geometry than that used by Kazemi [2]. De Swaan provided analytical solutions for early and late times in ideal spherical and plate reservoir models, but solutions for the transition period were not provided. Najurieta [4] enlarged the solutions provided by De Swaan [3] to include an accurate description of the transition period, focusing on transient behavior within the matrix. Najurieta [4] introduced a simple slab and cube model, and also recommended a methodical approach for interpreting well-test data in naturally fractured reservoirs. Bourdet-Gringarten [5] presented an improved group of type curves to analyze the effects of fluid storage in dual-porosity systems and expanded curves by restructuring the parameter sets according to the solutions provided by Mavor and Cinco-Ley [6]. Based on well test data, Gringarten et al. [7] also demonstrated how to apply the type curves to estimate matrix bulk volume and crack volume in fractured reservoirs. Utilizing pressure-derived type curves in well testing to interpret naturally fractured reservoirs proposed by Bourdet et al. [8]. An experimental design was used to analyze the sensitivity of reservoir performance, integrating geological and operational parameters, with a focus on improving reservoir management through statistical modeling. The key factors affecting production efficiency were highlighted and the predictive capabilities of complex reservoir systems were enhanced by Al-Mudhafer et al. [9]. Al-Hilali et al. [10] focused on the evaluation of permeability behavior in complex reservoirs using integrated petrophysical procedures and the flexibility of the introduced methodology to provide accurate reservoir characterization while Ali et al. [11] highlighted the characteristics of carbonate reservoirs in northern Iraq. Jie H. et al. [12] presented an innovative methodology for simulating fluid flow in fractured carbonate reservoirs, based on the transient Brinkman model. This iterative, physics-based approach aims to improve the accuracy of production predictions by focusing on fracture geometry rather than permeability, enhancing the accuracy of reservoir characterization and modeling. Silva-Escalante [13] used fractal modeling to characterize naturally fractured reservoirs by incorporating permeability and porosity distributions into simulations and focused on unique pressure responses and production scenarios, with a core on the influence of fractal dimensions on reservoir behavior, improving characterization and prediction capabilities for complex reservoirs.

2. Geological Setting

The Ellenberger Formation is the deepest oil-producing horizon in North Texas, is a secondary exploration target. Ellenberger oil production is characterized by the following features: (1) small structural features, (2) high gravity, typically above 40° API, (3) undersaturation, (4) associated water production, and (5) primary recovery of 25% of the initial oil in-situ. Although most of the oil remains unrecovered at the end of primary operations, secondary recovery techniques are currently uneconomical due to the small size of the structures and water flow. In reservoirs with large differences between matrix and fracture permeability, there may be potential to increase ultimate recovery by utilizing water absorption from fractures into the matrix, requiring alternating production and shutdown cycles. Figure (3) illustrates the structural map of the Ellenberger Formation.

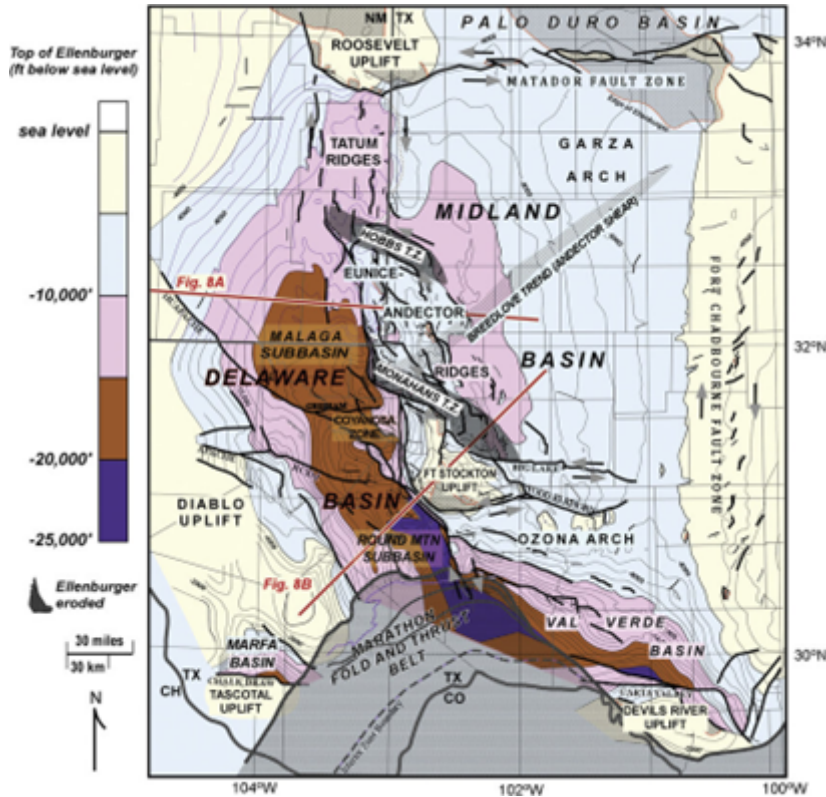


Figure 3. The structure map of the Ellenburger formation^[14]

3. Mathematical Modeling

According to the adopted model, the transfer of fluids from the matrix to the fracture system is supposed to occur under pseudo-steady conditions, while the total production of fluids within the reservoir is considered to take place exclusively through the fracture system, where the flow within this system is represented as a radial flow. This model matches with the Warren and Root model [1] and the diffusivity equation is modified as follows:

$$\frac{1}{r} \frac{\partial}{\partial r} \left(r \frac{k_f}{\mu} \frac{\partial p_f}{\partial r} \right) = \phi_f C_{tf} \frac{\partial p_f}{\partial t} + \phi_m C_{tm} \frac{\partial \bar{p}_m}{\partial t} \quad 1$$

The dimensionless pressure and time are expressed as:

$$p_{WD} = \frac{k_f h \Delta p}{\alpha_p q B \mu} \quad 2$$

$$t_D = \frac{\alpha_f k_f t}{(\phi_f C_{tf} + \phi_m C_{tm}) \mu r_{w2}^2} \quad 3$$

So, the diffusivity equation can be expressed in dimensionless form as:

$$\frac{1}{r_D} \frac{\partial}{\partial r_D} \left(\frac{\partial p_{Df}}{\partial r_D} \right) = \omega \frac{\partial p_{Df}}{\partial t} + (1 - \omega) \frac{\partial \bar{p}_{Dm}}{\partial t} \quad 4$$

The differential equation describing the flow in a matrix under pseudo-steady conditions is as follows:

$$\emptyset_m C_{tm} V_m \frac{\partial \bar{p}_m}{\partial t} = \frac{k_m}{\mu} A_m (\bar{p}_m - p_f) \quad 5$$

In dimensionless form, it becomes:

$$(1 - \omega) \frac{\partial \bar{p}_{Dm}}{\partial t} = \lambda (\bar{p}_{Dm} - p_{Df}) \quad 6$$

4. Results and Discussion

When the Ellenberger field was with an initial pressure of 5,000 psi and a reservoir temperature of 212°F. The initial gas-to-oil ratio (RSI) was for a 45° API 562 SCF/STB gravity crude, with a gas gravity of 0.7. Table 1 shows main PVT data for the Ellenberger field.

Table 1. Main PVT data of Ellenberger field.

Pressure (psia)	Z (λ)	Mug (cp)	Bg (cf/scf)	cg (psi-1)	Rhog (g/cc)	Temperatur e (°F)	Pb (psia)	Pressure (psia)	Rs (scf/stb)	Bo (B/STB)	co (psi-1)	Muo (cp)	Rhoo (g/cc)
14.6959	0.998758	0.013541	1.29007	0.068131	0.000665	68	1438.2	14.6959	5.1316	1.07763	0.035878	0.78561	0.743096
64.6959	0.99456	0.013562	0.291812	0.015541	0.002938	71.42	1448.72	64.6959	13.5903	1.08128	0.004183	0.757816	0.741781
114.696	0.990407	0.013592	0.163919	0.008802	0.00523	74.84	1459.33	114.696	23.1224	1.08542	0.001824	0.729934	0.740296
164.696	0.986302	0.013627	0.113678	0.006155	0.007542	78.26	1470	164.696	33.3919	1.08989	0.001079	0.703243	0.738691
214.696	0.982247	0.013666	0.086845	0.00474	0.009872	81.68	1480.76	214.696	44.2357	1.09465	0.000735	0.67815	0.736992
264.696	0.978244	0.01371	0.070154	0.003859	0.012221	85.1	1491.59	264.696	55.5551	1.09965	0.000542	0.654746	0.735215
314.696	0.974296	0.013757	0.058769	0.003258	0.014588	88.52	1502.5	314.696	67.2829	1.10486	0.000422	0.63299	0.733337
364.696	0.970405	0.013808	0.050509	0.002822	0.016974	91.94	1513.49	364.696	79.3703	1.11025	0.000341	0.612784	0.731465
414.696	0.966573	0.013862	0.044244	0.00249	0.019378	95.36	1524.56	414.696	91.78	1.11583	0.000283	0.594008	0.729507
464.696	0.962803	0.01392	0.03933	0.00223	0.021799	98.78	1535.71	464.696	104.482	1.12157	0.00024	0.576542	0.727502
514.696	0.959097	0.01398	0.035372	0.002019	0.024238	102.2	1546.94	514.696	117.453	1.12747	0.000207	0.560266	0.725453
564.696	0.955458	0.014044	0.032118	0.001846	0.026694	105.62	1558.24	564.696	130.673	1.13351	0.000181	0.545072	0.723365
614.696	0.951889	0.01411	0.029395	0.001701	0.029166	109.04	1569.63	614.696	144.124	1.13969	0.00016	0.53086	0.721241
664.696	0.948391	0.014179	0.027084	0.001577	0.031655	112.46	1581.11	664.696	157.792	1.14601	0.000143	0.517541	0.719085
714.696	0.944969	0.014252	0.025098	0.001471	0.03416	115.88	1592.66	714.696	171.665	1.15246	0.000128	0.505032	0.716898
764.696	0.941623	0.014326	0.023374	0.001378	0.036679	119.3	1604.3	764.696	185.731	1.15903	0.000116	0.493263	0.714684
814.696	0.938358	0.014404	0.021864	0.001296	0.039213	122.72	1616.02	814.696	199.981	1.16573	0.000106	0.482169	0.712445
864.696	0.935175	0.014485	0.02053	0.001224	0.041762	126.14	1627.82	864.696	214.406	1.17254	9.75E-05	0.471693	0.710183
914.696	0.932077	0.014568	0.019343	0.001159	0.044323	129.56	1639.71	914.696	228.997	1.17947	8.98E-05	0.461782	0.707901
964.696	0.929066	0.014654	0.018281	0.0011	0.046898	132.98	1651.69	964.696	243.749	1.1865	8.32E-05	0.452392	0.705599
1014.7	0.926146	0.014742	0.017326	0.001048	0.049484	136.4	1663.75	1014.7	258.653	1.19365	7.73E-05	0.44348	0.703281

4.1. Behavior of Dual-Porosity Model

4.1.1. Test History of Well #Az

Well # Az was chosen for simulation in this field, producing at a rate of 600 metric tons/day for 24 hours, then shut down for 48 hours, as shown in Figure 4. The values used in the simulation are: Omega = 0.52, Lambda = 1E-9, K = 3000 m3/day, and Re = 5000 ft.

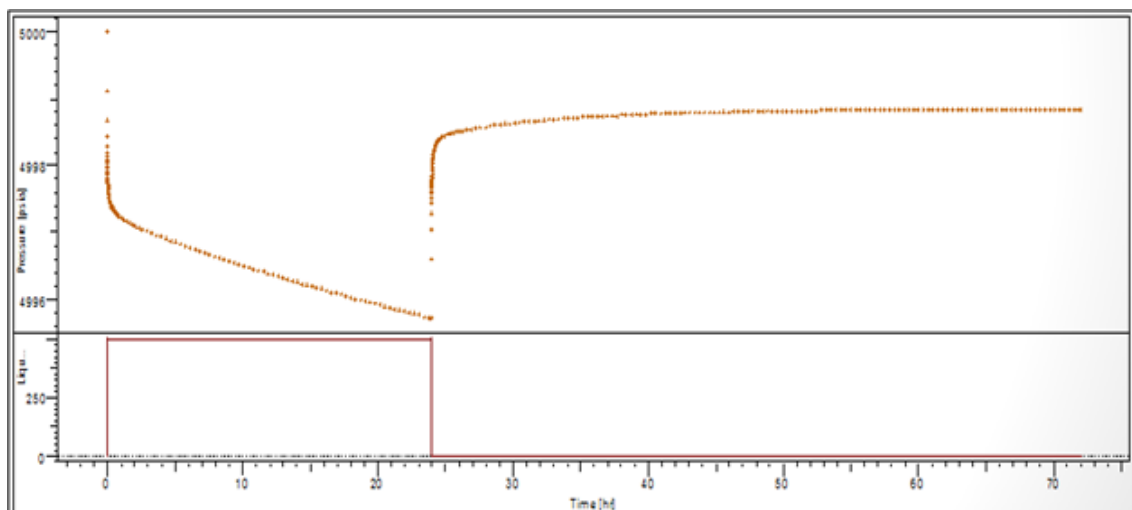


Figure 4. Reservoir pressure[psia], Rate of liqued [surface bbl/Day] vs. Time [hr]), history Plot

Omega values indicate a high fracture contribution to storage capacity, and the value of lambda indicates a high fracture contribution to flow capacity.

4.2. Drawdown Test

Figures 5 and 6 show the results of the pull test fit.

Where the values are:

$C = 0.0145 \text{ bbl/sq. in}$, Skin = -0.0195, initial reservoir pressure = 5000 psi, $k \cdot h = 1.5E + 5 \text{ md.ft}$, $k = 3000 \text{ mdarcy}$, Omega = 0.486, Lambda = 1.03E-9.

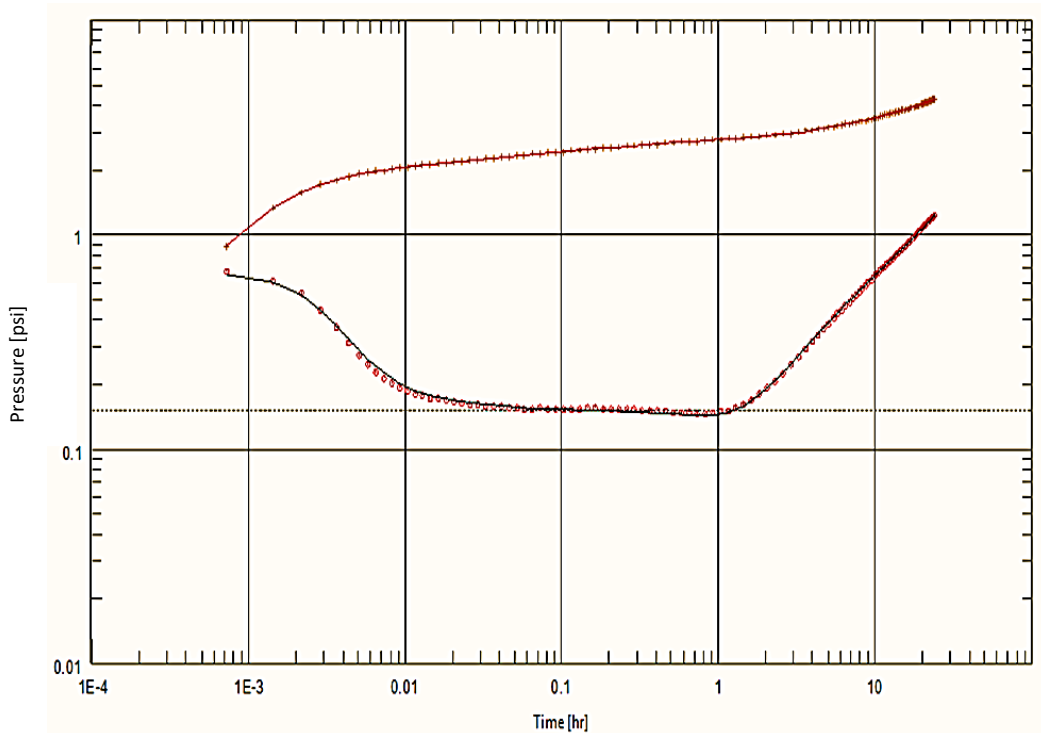


Figure 5. Log-Log Plot :P-P@dt=0, Derivative [psia] vs dt [hr]

Figure 5 (Log-Log) shows a perfect fit of the curves, with no V-shape in the signal due to the matrix feed approaching zero. The behavior appears similar to that in a finite homogeneous reservoir.

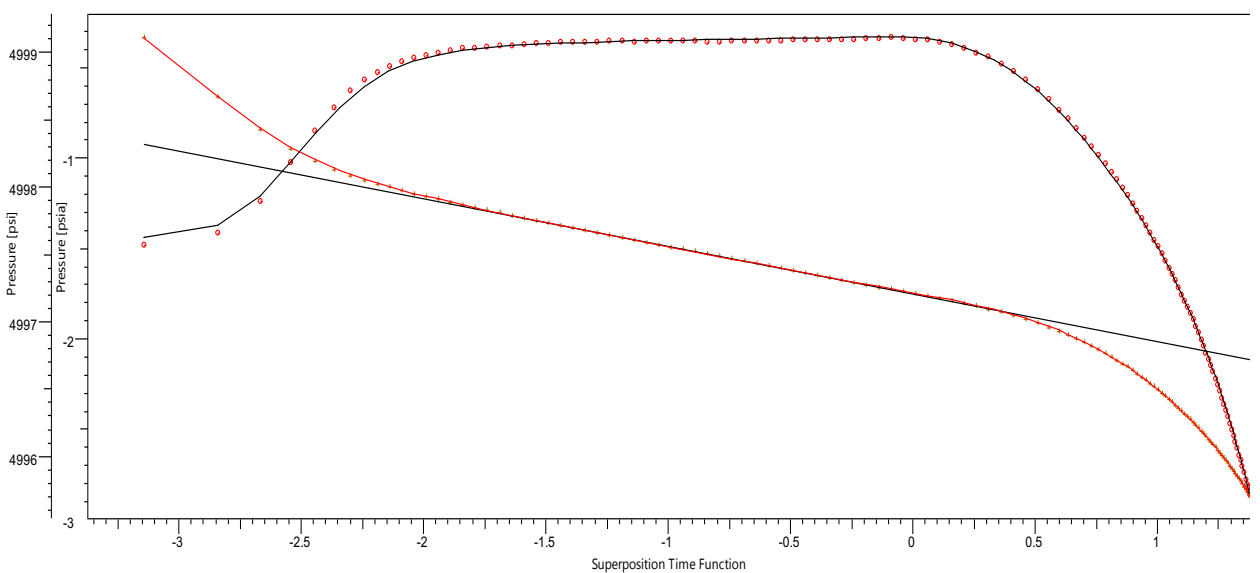


Figure 6. MDH Plot : P [psi], Derivative [psia] vs log(dt)

Figure 6 (Semi-Log) shows a perfect fit to the curves and shows two pseudo-straight lines as shown in the derivative curve. The behavior appears similar to that in a finite homogeneous reservoir.

4.3. Buildup Test

Figure 7 shows the matching results for build up log-log plot;

Where the values are:

Re-no flow=5650 ft, Initial reservoir pressure=5000 psi, $K \cdot h = 1.49E+5$ md.ft, $K = 2980$ mdarcy, $\Omega = 0.494$, $\Lambda = 1.01E-9$.

Figure 7 (Log-Log) shows the perfect matching of curves and the V-shape signature reflecting boundary effects.

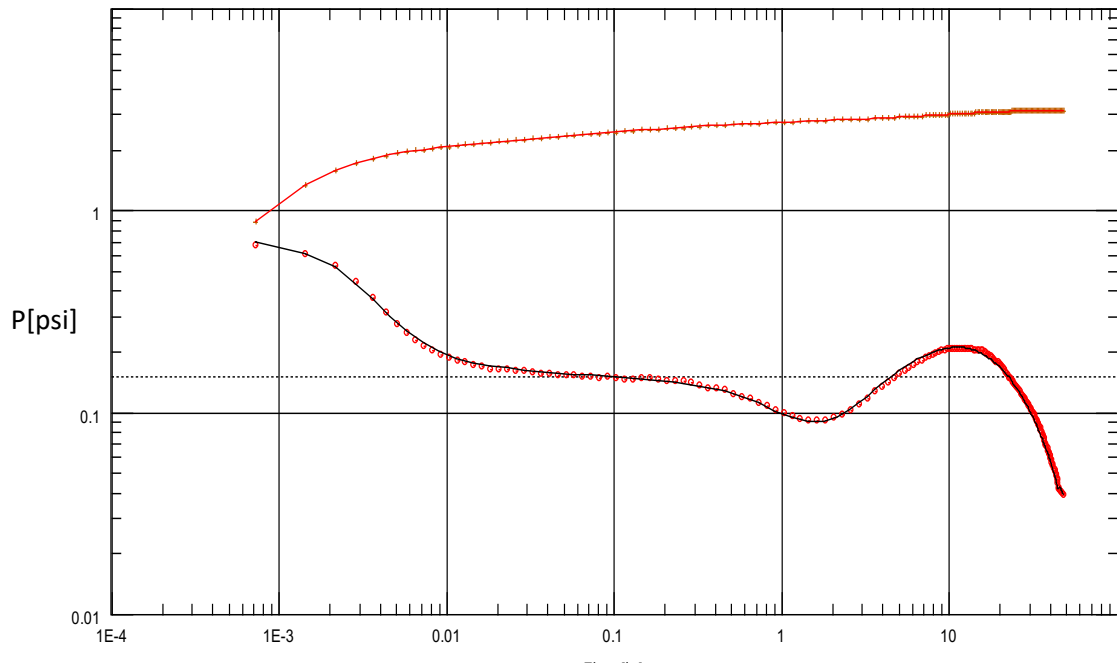


Figure 7. Log-Log plot: p-p @ $dt = 0$, Derivative [psi] vs dt [hr]

Figure 8 and 9 show the matching results for build up semi-log Horner plot;

Skin=5.99, $K \cdot h = 2.51E+5$ md.ft, $K = 5020$ mdarcy, $\Omega = 0.271$, $\Lambda = 1.68E-10$.

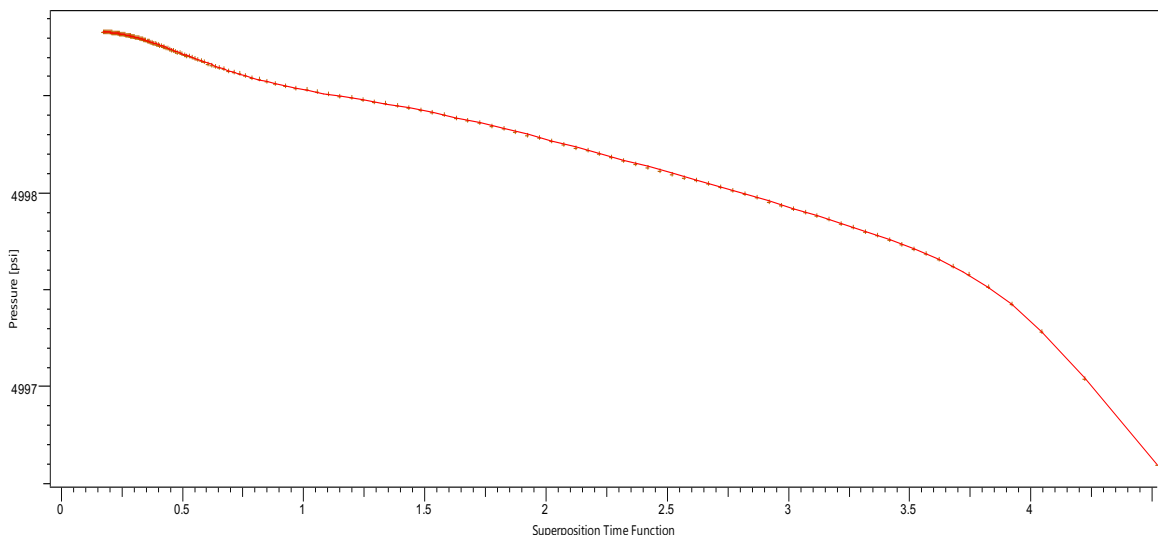


Figure 8. Hornerplot: reservoir pressure [psi] vs $\log(tp+dt)-\log(dt)$

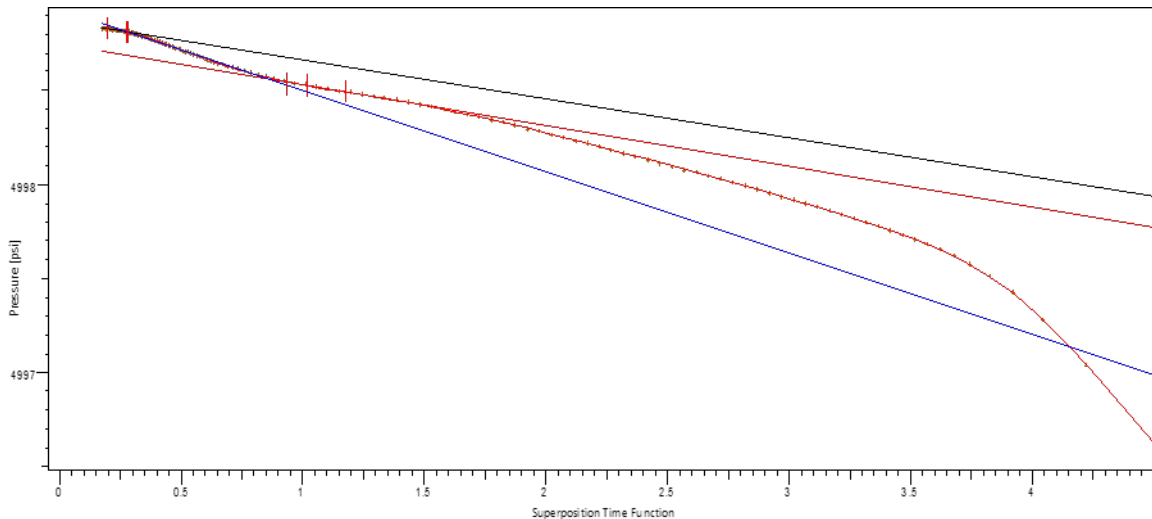


Figure 9. Hornerplot:reservoir pressure [psi] vs $\log(tp+dt)-\log(dt)$

Semi-log plot shows wrong straight lines identification leads to enormously erroneous results.

5. Conclusions

1. The semi-logarithmic straight line should be treated with caution, as the effects of boundaries and well storage in heterogeneous and bounded reservoirs may manifest similarly.
2. Homogeneous models with bounded boundaries do not exhibit Type I behavior, making the application of return models impossible.
3. A prominent V-shape is clearly observed when analyzing well tests, indicating that the fractures in this field are Type I.
4. Fitting model curves with derivatives is an effective tool for analyzing all types of reservoirs with natural fractures.
5. The same behavior can be modeled using different approaches, depending on the nature of the reservoir and the available data.

References

1. Warren, J.E., Root, P.J., 1963 .The Behavior of Naturally Fractured Reservoirs. SPE J. 3 (03): 245–255, SPE-426-PA. <https://doi.org/10.2118/426-PA>.
2. Kazemi, H., 1969. Pressure Transient Analysis of Naturally Fractured Reservoirs with Uniform Fracture Distribution, SPE J. 9 (04): 451–462. <https://doi.org/10.2118/2156-A>.
3. De Swaan O., A., 1976. Analytic Solutions for Determining Naturally Fractured Reservoir Properties by Well Testing. SPE J. 16 (03): 117–122, SPE-5346-PA. <https://doi.org/10.2118/5346-PA>.
4. Najurieta H. L., 1980. A Theory for Pressure Transient Analysis in Naturally Fractured Reservoirs. J Pet Technol 32 (07): 1241–1250. SPE-6017-PA. <https://doi.org/10.2118/6017-PA>.
5. Bourdet, D., Gringarten, A.C., 1980. Determination of Fissure Volume and Block Size in Fractured Reservoirs by Type-Curve Analysis, SPE-9293-MS. <https://doi.org/10.2118/9293-MS>.
6. Mavor, M.J. and Cinco-Ley H., 1979. Transient Pressure Behavior of Naturally Fractured Reservoirs. SPE California Regional Meeting, Ventura, California, SPE-7977-MS. <https://doi.org/10.2118/7977-MS>.

7. Gringarten, A.C., et al., 1979. A Comparison Between Different Skin and Wellbore Storage type-Curves for Early time Transient Analysis. SPE 8205, Annual Technical Conference and Exhibition, Las Vegas, Nevada. <https://doi.org/10.2118/8205-MS>.
8. Bourdet, D., Alagoa, A., Ayoub, J.A., Pirard, Y.M., Melun, J., 1984. New Type Curves Aid Analysis of Fissured Zone Well Tests, World Oil, April, 111. ISSN:0043-8790.
9. Al-Mudhafer W.J.M., Zein Al- Abideen M.J., 2014. Experimental Design for Sensitivity Analysis of Reservoir Performance - Case Study. European Association of Geoscientists & Engineers Source: , 6th EAGE Saint Petersburg International Conference and Exhibition, <https://doi.org/10.3997/2214-4609.20140251>.
10. Al-Hilali, M.M., Al-Abideen, M.J.Z., Adegbola, F., Avedisian, A.M. 2015. A Petrophysical Procedure to Evaluate Permeability Behavior in Complex Reservoirs; Case studies in IRAQI Oilfields, SPE-177332-MS, SPE Annual Caspian Technical Conference and Exhibition. <https://doi.org/10.2118/177332-MS>.
11. Ali, Ghassan H., Yahya J. Tawfeeq, and Mohammed Y. Najmuldeen, 2019. Comparative Estimation of Water Saturation in Carbonate Reservoir: A Case Study of Northern Iraq. Periodicals of Engineering and Natural Sciences (PEN) 7(4): 1743-1754. <https://doi.org/10.21533/pen.v7.i4>.
12. Jie He, John E. Killough, Sunhua Gao, Mohamed M. Fadlelmula, F. Michael Fraim, 2016. SPE-183143-MS, Confronting the Simulation of Fluid Flow in Naturally Fractured Carbonate Karst Reservoirs. Abu Dhabi International Petroleum Exhibition & Conference. <https://doi.org/10.2118/183143-MS>
13. Silva-Escalante C.F., Camacho-Velazquez R.G., 2024. SPE Western Regional Meeting, SPE-218949-MS. <https://doi.org/10.2118/218949-MS>
14. Fairhurst Bill, Ewing Tom, Lindsay Bob, 2021. West Texas (Permian) Super Basin, United States: Tectonics, structural development, sedimentation, petroleum systems, and hydrocarbon reserves. AAPG Bulletin 105(6):1099-1147. <https://doi.org/10.1306/03042120130>.
15. Tawfeeq Y. J., Najmuldeen M. Y., and Ali G. H., 2020. Optimal statistical method to predict subsurface formation permeability depending on open hole wireline logging data: A comparative study. Periodicals of Engineering and Natural Sciences, 8, 2, 736–749. <https://doi.org/10.21533/pen.v8.i2>.